Paper

Dynamic Available Transfer Capability Evaluation by Interior Point Nonlinear Programming

Yue Yuan* Member
Junji Kubokawa** Member
Hiroshi Sasaki*** Member

In nowadays deregulated market, available transfer capability (ATC) is a measure of the network capability for further commercial activity above the already committed uses. This paper deals with the development of an interior point nonlinear programming methodology for evaluating dynamic ATC. By establishing a novel method for integrating transient stability constraints into conventional steady-state ATC problem, the dynamic ATC problem is successfully formulated as an OPF-based optimization problem. Then, an interior point nonlinear programming algorithm is used to solve the formed dynamic ATC optimization problem. The method has been implemented and tested on two IEEJ model systems (WEST10 and WEST30). In both systems, satisfactory results are obtained.

Keywords: available transfer capability, interior point method, nonlinear programming, optimal power flow, transient stability

1. Introduction

Recent years, electric power systems are experiencing an epochal revolution due to an increasingly competitive market. Also in Japan, the Electric Industry Law was amended in 1995 aiming to deregulate the wholesale electricity supply business. Under such an open transmission access environment, it is more and more important for the system operator to know how much additional power can be safely transferred across the system.

Available Transfer Capability (ATC) is the measure of the ability of interconnected electric systems to reliably transfer power from one area to another over all transmission lines or paths between those areas under specified system conditions. In nowadays deregulated market, it is a measure of the network capability for further commercial activity above the already committed uses.

Until now, ATC calculation has predominantly focussed on steady-state viability [1]. In the dynamic realm, evaluation of ATC including voltage stability limits has also been considered [2]. However, the integration of transient stability constraints into ATC calculation is still a relatively new development. Especially, few OPF-based dynamic ATC algorithms are available although they are conceptually rather nice [3].

Reference (11) first pointed out the possibility of calculating ATC by means of stability-constrained OPF. Then, using a total different method, Ref. (12) formulated transient stability-constrained ATC. Also in Ref. (12), simulation results of a one-machine-infinite-bus system and a two-machine-four-bus system were given.

In fact, the literature on ATC calculation is rich. Some excellent works published in IEEJ Journal or Conference Publication include [12]~[14]. All these methods, including the one we presented in this paper, are in developing stages. It is not difficult to formulate these problems. However, with more limits (thermal, voltage, and/or stability) are taken into consideration, it is very challenging in the implementation.

This paper deals with the development of an interior point nonlinear programming methodology for evaluating dynamic ATC. The main features of the approach are:

- By establishing a novel method for integrating transient stability constraints into conventional steady-state ATC (S-ATC) problem, the dynamic ATC (D-ATC) problem is successfully formulated as an OPF-based optimization problem.
- Unlike most of the linear programming (LP) methods used in S-ATC, a methodology based on primal-dual Newton interior point method (IPM) for nonlinear programming (NLP) problems is introduced to solve the formed D-ATC optimization problem.

The method has been implemented in FORTRAN language and has been tested on two IEEJ model systems (WEST10 and WEST30). In both systems, satisfactory results are obtained with acceptable computation time. Furthermore, in all cases, dynamic responses obtained by our D-ATC are verified by the widely-used CRIEPI's power system dynamic stability analysis program.

* College of Electrical Engineering, Hohai University
Nanjing, China
** Department of Information and Intellectual Systems Engineering, Hiroshima Institute of Technology
2-1-1, Miyake, Saeki-ku, Hiroshima 731-5193
*** Department of Electrical Engineering, Hiroshima University
1-4-1, Kagamiyama, Higashi-Hiroshima 739-8527

2. ATC Definition and Determination

Generally speaking, the term "available transfer capability" refers to the amount of electric power that interarea bulk power transfers can be increased without compromising system security. In this study, we use the main features of the NERC 1996 definitions [4]: The power system is judged to be secure for the purpose of interarea transfer if "all facility loadings are within normal ratings and all voltages are within normal limits", the system "remains stable following a disturbance that results in the loss of any single electric system elements, such as a transmission line, transformer, or generator unit", the post-contingency system as all facility loadings within emergency ratings and all voltages within emergency limits.

For ATC evaluation, first a base case transfer including existing transmission commitments is chosen. Then a transfer limited case is determined. Mathematically, ATC is defined as:

$$\begin{aligned}\text{ATC} = {} & \text{Total Transfer Capability (TTC)} \\ & \text{Existing Transmission Commitments (ETC)} \\ & \text{Transmission Reliability Margin (TRM)} \\ & \text{Capacity Benefit Margin (CBM)}\end{aligned} \quad \cdots\cdots\cdots\cdots\cdots\cdots (1)$$

TTC is defined as the amount of electric power that can be transferred over an interface or a corridor of the interconnected transmission network in a reliable manner while meeting all of a specific set of defined pre- and post-contingency system conditions. TRM is defined as that amount of transmission transfer capability necessary to ensure that the interconnected network is secure under a reasonable range of uncertainties in system conditions. CBM is defined as that amount of transmission transfer capability reserved by load serving entities to ensure access to generation from interconnected systems to meet generation reliability requirements.

Since TRM and CBM are very system dependent, in this paper, we address the calculation of TTC, which is at the basis of ATC evaluation.

3. Mathematical Formulation of Transient Stability Constraints used in D-ATC

3.1 Power System Model for Transient Stability Constrained D-ATC In our study, the classical power system model for transient stability analysis is adopted. The so-called classical model based on the following simplifying assumptions [5]:

(a) The synchronous machine is represented by a voltage source of constant magnitude E'_i determined from the pre-fault steady-state conditions, in series with a reactance x'_{di} which is commonly called the direct axis transient reactance. And the phase angle of the voltage behind transient reactance coincides with the rotor angle δ_i.

(b) Loads are represented as constant impedances based on the pre-fault voltage conditions.

(c) The mechanical input power is assumed to be constant and equal to the pre-fault value during the time interval of interest which is of the order of 1–2 sec.

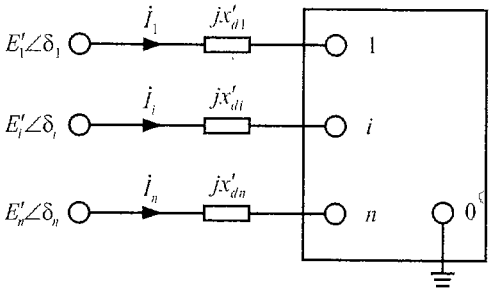

Fig. 1. Classical power system model

In this case, the swing equation set (equations of motion) is:

$$\left.\begin{aligned}\dot{\delta}_i &= \omega_i - \omega_0 \\ M_i\dot{\omega}_i &= \omega_0(-D_i\omega_i + P_{mi} - P_{ei}) \\ & (i = 1, 2, \cdots, ng)\end{aligned}\right\} \cdots\cdots\cdots (2)$$

where

δ_i: rotor angle of i-th generator
ω_i: rotor speed of i-th generator
M_i: inertia constant of i-th generator
D_i: damping constant of i-th generator
P_{mi}: mechanical input power of i-th generator
P_{ei}: electrical output power of i-th generator
ω_i: synchronous speed
ng: number of generators

With the above assumptions, we can proceed to derive an analytic expression P_{ei} for in terms of δ_i's.

Assume the transmission network to consist of $ng+nl$ buses of which the first ng buses are buses where generators are connected and at the other nl buses only loads are connected. Then, the nodal admittance matrix of this network can be given by:

$$\mathbf{Y} = \begin{bmatrix}\mathbf{Y}_{GG} & \mathbf{Y}_{GL} \\ \mathbf{Y}_{LG} & \mathbf{Y}_{LL}\end{bmatrix} \cdots\cdots\cdots\cdots\cdots\cdots\cdots (3)$$

Each of the generator buses is now augmented by the generator representation as assumption (a). Fig. 1 shows the topology of the network. Number the internal buses of the generators as $1, 2, \cdots, ng$ and the transmission network buses as $ng+1, \cdots, 2ng+nl$, we have:

$$\begin{bmatrix}\dot{\mathbf{I}}_G \\ \mathbf{0} \\ \mathbf{0}\end{bmatrix} = \begin{bmatrix}\mathbf{Y}_G & -\mathbf{Y}_G & \mathbf{0} \\ -\mathbf{Y}_G & \mathbf{Y}_G + \mathbf{Y}_{GG} & \mathbf{Y}_{GL} \\ \mathbf{0} & \mathbf{Y}_{LG} & \mathbf{Y}_{LL}\end{bmatrix} \begin{bmatrix}\dot{\mathbf{E}}' \\ \dot{\mathbf{U}}_G \\ \dot{\mathbf{U}}_L\end{bmatrix} \cdots\cdots (4)$$

where

$\dot{\mathbf{I}}_G$: injected current vector
$\dot{\mathbf{E}}'$: generator internal voltage vector
$\dot{\mathbf{U}}_G$: network generator bus terminal voltage vector
$\dot{\mathbf{U}}_L$: network load bus terminal voltage vector
$\mathbf{Y}_G$: diagonal matrix with the element $1/jx'_{di}$

From the stability point of view, we are primarily interested in the variation of δ_i as a function of time and not the bus voltages. For this reason, we now eliminate

all buses except the generator internal buses. Then, we have the following equations:

$$\dot{\mathbf{I}}_G = \mathbf{Y}_{E'}\dot{\mathbf{E}}' \quad \cdots\cdots (5)$$

where

$$\mathbf{Y}_{E'} = \mathbf{Y}_G - \begin{bmatrix} -\mathbf{Y}_G & \mathbf{0} \end{bmatrix} \begin{bmatrix} \mathbf{Y}_G + \mathbf{Y}_{GG} & \mathbf{Y}_{GL} \\ \mathbf{Y}_{LG} & \mathbf{Y}_{LL} \end{bmatrix}^{-1} \begin{bmatrix} -\mathbf{Y}_G \\ \mathbf{0} \end{bmatrix}$$

Let elements of this $\mathbf{Y}_{E'}$ matrix be noted by $Y'_{ij} = G'_{ij} + B'_{ij}$ $(i, j = 1, 2, \cdots, ng)$. Y'_{ij} is the driving point admittance or the transfer admittance $(i = j)$ at the internal buses $(i \neq j)$. It is obvious that $\mathbf{Y}_{E'}$ is a symmetrical matrix and in most cases not a sparse matrix.

Equation (5) is the internal bus description of the system. Although it masks the topological aspects, it simplifies the analysis considerably in terms of obtaining an analytic expression for P_{ei} in swing Eq. (2). The expression for real power generation is:

$$\begin{aligned} P_{ei} &= Re(\dot{E}'_i I_i^*) \\ &= \mathrm{Re}\left(\dot{E}'_i \sum_{j=1}^{ng} Y'^*_{ij} E'^*_j\right) \\ &= E'^2_i G'_{ii} + \sum_{j=1, j\neq i}^{ng} [C_{ij}\sin(\delta_i - \delta_j) + D_{ij}\cos(\delta_i - \delta_j)] \end{aligned} \quad \cdots\cdots (6)$$

where

$$\left.\begin{aligned} C_{ij} &= C_{ji} = E'_i E'_j B'_{ij} \\ D_{ij} &= D_{ji} = E'_i E'_j G'_{ij} \end{aligned}\right\} i, j = 1, 2, \cdots, ng; j \neq i$$

It should be noted that, owing to the differences of nodal admittance matrices $\mathbf{Y}$ during the pre-fault, fault-on, and post-fault stages, G'_{ij} and B'_{ij} need to do corresponding modifications.

As existing optimization methods cannot directly deal with the kind of problem which contains both algebraic and differential equation constraints, our activity is to discretize differential equation set (2) to form algebraic equations which can easily be incorporated into optimization problems as additional constraints. By the adoption of trapezoidal rule, an excellent implicit integration method recommended by Ref. (6) for power system transient stability numerical solution, the swing equation set (2) can be discretized at each time step to form the following numerically equivalent algebraic equations:

$$\left.\begin{aligned} &\delta_i^{t+1} - \delta_i^t - \frac{\Delta t}{2}[(\omega_i^t - \omega_0) + (\omega_i^{t+1} - \omega_0)] = 0 \\ &\omega_i^{t+1} - \omega_i^t - \frac{\Delta t}{2}\frac{\omega_0}{M_i}[(-D_i\omega_i^t + P_{mi} - P_{ei}^t) \\ &\quad + (-D_i\omega_i^{t+1} + P_{mi} - P_{ei}^{t+1})] = 0 \\ &\quad (i = 1, 2, \cdots, ng; t = 0, 1, \cdots, nt) \end{aligned}\right\} \quad \cdots\cdots (7)$$

where

$$P_{ei}^t = E'^2_i G'^t_{ii} + \sum_{\substack{j=1 \\ \neq i}}^{ng} [C_{ij}^t \sin(\delta_i^t - \delta_j^t) + D_{ij}^t \cos(\delta_i^t - \delta_j^t)]$$

$$C_{ij}^t = E'_i E'_j B'^t_{ij}, D_{ij}^t = E'_i E'_j G'^t_{ij}; t = 0, 1, \cdots, nt$$

Δt is integration step-width

n is the number of integration time intervals

3.2 Initial Value Calculation Prior to the disturbance, the power system is in a steady state with constant values δ_i^0 and $\delta_i = 0$. E'_i and δ_i^0 are computed by the knowing voltages at the generator buses and the scheduled generations from the power flow data. The initial-value equations are:

$$\left.\begin{aligned} &E'_i V_{gi}\sin(\delta_i^0 - \theta_{gi}) - x'_{di} P_{gi} = 0 \\ &V_{gi}^2 - E'_i V_{gi}\cos(\delta_i^0 - \theta_{gi}) + x'_{di} Q_{gi} = 0 \\ &\quad (i = 1, 2, \cdots, ng) \end{aligned}\right\} \cdots\cdots (8)$$

where

$V_{gi}\angle\theta_{gi}$: voltage $\dot{V}_{gi}$ at generator bus i

P_{gi}, Q_{gi}: active and reactive power generations at bus i

3.3 Transient Stability Constraints Transient stability for various contingency conditions are ensured by introducing a suitable criterion. In this study, we use the conventional maximum relative rotor angle criterion, in which rotor angles with respect to Center of Inertia (COI) are measured [7]. Under this definition, transient stability constraints can be formulated as:

$$\left.\begin{aligned} &\underline{\delta} \leq \delta_i^t - \delta_{COI}^t \leq \bar{\delta} \\ &\delta_{COI}^t = \sum_{i=1}^{ng} M_i \delta_i^t \Big/ \sum_{i=1}^{ng} M_i \\ &(i = 1, 2, \cdots, ng; t = 0, 1, \cdots, nt) \end{aligned}\right\} \cdots\cdots (9)$$

where

δ_{COI}: position of the COI

$\bar{\delta}, \underline{\delta}$: upper and lower limit of rotor angles w.r.t. COI

4. Formulation of Dynamic TTC Problem

As shown in Fig. 2, an interconnected power system can be divided into three kinds of areas: sending areas, receiving areas and external areas. "Area" can be defined in an arbitrary fashion. It may be an individual electric system, power pool, control area, subregion, etc.

The objective of a TTC problem is to determine the maximum real power transfers from sending areas to receiving areas through the transfer paths. And the physical and electrical characteristics of the systems limiting the transfer capability include:

(a) Generation limits: Generation should not over the rated output of each generation unit.

(b) Voltage limits: Voltages over the transmission system should be within acceptable operation ranges.

(c) Thermal limits: Constrain the amount of transfer that transmission line can be safely handle without overload.

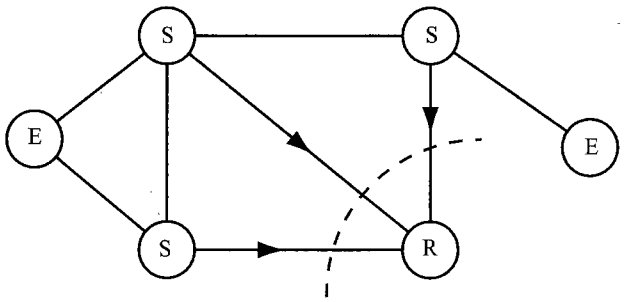

Fig. 2. A simple interconnected power system

(d) Stability limits: Voltage stability and angle stability must be maintained.

In short, the TTC is given by:

$$\begin{aligned}\text{TTC} = &\text{ Minimum of Generation limits,}\\ &\text{Voltage limits, Thermal limits,}\\ &\text{Stability limits} \cdots\cdots\cdots\cdots\cdots\cdots (10)\end{aligned}$$

In most electric systems of Japan, angle stability limits are the crucial factors that determine transmission limits [8]. On considering this point, to simplify TTC calculation, we assume that bus voltage limits are reached before the system reaches the nose point and loses voltage stability. Hence, voltage stability limits are neglected in this study. The calculation of TTC in this case can be formulated as an optimal power flow problem as follows:

Minimize A scalar objective function:

$$\left.\begin{aligned}P_T &= \sum_{i\in S_{SA}, j\in S_{RA}} P_{ij}\\ P_{ij} &= G_{ij}V_i^2 - V_iV_j(G_{ij}\cos\theta_{ij} + B_{ij}\sin\theta_{ij})\end{aligned}\right\} \cdots\cdots\cdots\cdots\cdots (11)$$

Subject to:

Inequality constraints:

$$\left.\begin{aligned}&\underline{P}_{gi} \le P_{gi} \le \bar{P}_{gi} && (i \in S_G)\\ &\underline{Q}_{gi} \le Q_{gi} \le \bar{Q}_{gi} && (i \in S_R)\\ &\underline{V}_i \le V_i \le \bar{V}_i && (i \in S_N)\\ &\underline{P}_{ij} \le P_{ij} \le \bar{P}_{ij} && ((i,j) \in S_{CL})\\ &\underline{\delta} \le \delta_i^t - \delta_{COI}^t \le \bar{\delta} && (i \in S_G; t \in S_T)\end{aligned}\right\} \cdots\cdots (12)$$

Equality constraints:

$$\left.\begin{aligned}&P_{gi} - P_{li} - \sum_{j=1}^{nb} V_iV_jY_{ij}\cos(\theta_i - \theta_j - \alpha_{ij}) = 0\\ &Q_{gi} - Q_{li} - \sum_{j=1}^{nb} V_iV_jY_{ij}\sin(\theta_i - \theta_j - \alpha_{ij}) = 0\end{aligned}\right\} i \in S_N$$

$$\left.\begin{aligned}&\delta_i^{t+1} - \delta_i^t - \frac{\Delta t}{2}[(\omega_i^t - \omega_0) + (\omega_i^{t+1} - \omega_0)] = 0\\ &\omega_i^{t+1} - \omega_i^t - \frac{\Delta t}{2}\frac{\omega_0}{M_i}[(-D_i\omega_i^t + P_{mi} - P_{ei}^t) + (-D_i\omega_i^{t+1} + P_{mi} - P_{ei}^{t+1})] = 0\end{aligned}\right\} \begin{aligned}&i \in S_G\\ &t \in S_T\end{aligned}$$

$$\left.\begin{aligned}&E_i'V_{gi}\sin(\delta_i^0 - \theta_{gi}) - x_{di}'P_{gi} = 0\\ &V_{gi}^2 - E_i'V_{gi}\cos(\delta_i^0 - \theta_{gi}) + x_{di}'Q_{gi} = 0\end{aligned}\right\} i \in S_G \quad \cdots\cdots\cdots\cdots (13)$$

where

P_{ij}: active power of transmission line (i,j)

P_{li}, Q_{li}: active and reactive power loads at bus i

$V_i\angle\theta_i$: magnitude and phase of voltage $\dot{V}_i$ at bus i

S_{SA}: set of sending areas (SA)

S_{RA}: set of receiving areas (RA)

S_G: set of active power sources

S_R: set of reactive power sources

S_N: set of buses

S_{CL}: set of constrained transmission lines

S_T: set of integration steps

nb: number of buses

$Y_{ij}\angle\alpha_{ij}$: (i,j)-th element of the system admittance matrix

5. Formulation of Interior Point Algorithm for Dynamic TTC

5.1 Formulation of Algorithm [9] Assume that x is defined as a $n \times 1$ vector:

$$x \equiv \left[x^{control}\,\middle|\,x^{state}\right]^T \in R^n$$

Then, a Dynamic TTC problem may be formulated as the following NLP problem:

$$\left.\begin{aligned}&\text{minimize } f(x)\\ &\text{subject to } h(z) = 0\\ &\qquad \underline{g} \le g(x) \le \bar{g}\end{aligned}\right\} \cdots\cdots\cdots\cdots\cdots\cdots (14)$$

where $h(x) \equiv [h_1(x), \cdots, h_m(x)]^T$, $g(x) \equiv [g_1(x), \cdots, g_r(x)]^T$.

By introducing slack variable vectors $l, u \in R^r$, system (14) can be transformed to:

$$\left.\begin{aligned}&\text{minimize } f(x)\\ &\text{subject to } h(x) = 0\\ &\qquad g(x) - \underline{g} - l = 0; g(x) - \bar{g} + u = 0\\ &\qquad (l,u) \ge 0\end{aligned}\right\} \cdots\cdots\cdots\cdots\cdots (15)$$

Define a Lagrangian function associated with Eq. (15) as:

$$\begin{aligned}&L(x,l,u;y,z,w,\tilde{z},\tilde{w})\\ &\quad \equiv f(x) - y^Th(x) - z^T[g(x) - \underline{g} - l]\\ &\qquad - w^T[g(x) - \bar{g} + u] - \tilde{z}^Tl - \tilde{w}^Tu \cdots\cdots (16)\end{aligned}$$

where $y \in R^m$ and $z, w, \tilde{z}, \tilde{w} \in R^r$ are Lagrange multipliers.

$$\tilde{z} = z, \tilde{w} = -w.$$

Based on the perturbed Karush-Kuhn-Tucker (KKT) optimality conditions, we have the following equations:

$$\left.\begin{array}{l} L_x \equiv \nabla f(x) - \nabla h(x)y - \nabla g(x)(z+w) = 0 \\ L_l \equiv LZe - \mu e = 0 \\ L_u \equiv UWe + \mu e = 0 \\ L_y \equiv h(x) = 0 \\ L_z \equiv g(x) - \underline{g} - l = 0 \\ L_w \equiv g(x) - \bar{g} + u = 0 \\ (l,u) \geq 0, y \neq 0, z \geq 0 \ \& \ w \leq 0 \end{array}\right\} \quad \cdots\cdots\cdots\cdots\cdots (17)$$

where $L, U, Z, W \in R^{r \times r}$ are diagonal matrices with the element l_i, u_i, z_i and w_i. $\mu > 0$ is a perturbed factor. $e = [1, \cdots, l]^T \in R^r$.

By applying Newton's method to the perturbed KKT Eq. (16), the correction equation can be expressed as:

$$\left.\begin{array}{l} \left[\sum_{i=1}^{m} y_i \nabla^2 h_i(x) + \sum_{j=1}^{r}(z_j + w_j)\nabla^2 g_j(x) - \nabla^2 f(x)\right] \\ \quad \times \Delta x + \nabla h(x)\Delta y + \nabla g(x)(\Delta z + \Delta w) = L_{x0} \\ Z\Delta l + L\Delta z = -L^{\mu}_{l0} \\ W\Delta u + U\Delta w = -L^{\mu}_{u0} \\ \nabla h(x)^T \Delta x = -L_{y0} \\ \nabla g(x)^T \Delta x - \Delta l = -L_{z0} \\ \nabla g(x)^T \Delta x + \Delta u = -L_{w0} \end{array}\right\} \quad \cdots\cdots\cdots\cdots\cdots (18)$$

where $(L_{x0}, L^{\mu}_{l0}, L^{\mu}_{u0}, L_{y0}, L_{z0}, L_{w0})$ are the values at a point of expansion and denote the residuals of the perturbed KKT equations. $\nabla^2 f(x)$, $\nabla^2 h_i(x)$ and $\nabla^2 g_j(x)$ are Hessian matrices of $f(x)$, $h_i(x)$ and $g_j(x)$.

5.2 Reduction of Correction Equation In order to handle inequality constraints efficiently, a reduced correction equation is introduced. This reduction method is very effective for Dynamic TTC problem.

By eliminating $(\Delta l, \Delta u, \Delta z, \Delta w)$ from Eq. (17), we can derive the following reduced correction equation:

$$\begin{bmatrix} H(\square) & J(x^T) \\ J(x) & 0 \end{bmatrix} \begin{bmatrix} \Delta x \\ \Delta y \end{bmatrix} = - \begin{bmatrix} \Psi(\square, \mu) \\ \phi \end{bmatrix} \cdots\cdots (19)$$

where

$$\begin{aligned} H(\square) &\equiv H_1 + H_2 \\ &= \left[\sum_{i=1}^{m} y_i \nabla^2 h_i(x) + \sum_{j=1}^{r}(z_j + w_j)\nabla^2 g_j(x) - \nabla^2 f(x)\right] \\ &\quad + \sum_{j=1}^{r}\left(\frac{w_j}{u_j} - \frac{z_j}{l_j}\right)\nabla g_j(x)\nabla g_j(x)^T \\ J(x) &\equiv \nabla h(x)^T \\ \psi(\square, \mu) &\equiv \nabla h(x)y - \nabla f(x) + \nabla g(x)[U^{-1}WL_{w0} \\ &\quad - L^{-1}ZL_{z0} - \mu(U^{-1} - L^{-1})e] \\ \phi &\equiv h(x) \end{aligned}$$

It is obvious that the reduced correction equation has eliminated both variable inequality constraints and functional inequality constraints. The size of Eq. (18), which is determined only by the number of variables and equality constraints, is much smaller than that of Eq. (17).

5.3 Flow Chart of the Algorithm

Initialization: Set iteration counter $k = 0$; define centering parameter $\sigma \in (0, 1]$ and tolerance $\varepsilon = 10^{-6}$; chose a starting point for primal variables and dual variables.

Begin: $k = 0, 1, \cdots$

Step 1: (Test for Convergence)

Compute complementary gap:

$$CGAP_k \equiv \sum_{m=1}^{r}(l_m z_m - u_m w_m) \cdots\cdots\cdots\cdots (20)$$

If the operating point satisfied the convergence criteria $(CGAP_k) < \varepsilon$, then output the optimal solution and stop. Otherwise, do Step 2 to Step 5.

Step 2: (Compute the Perturbed Factor)

$$\mu_k \equiv \sigma \frac{CGAP_k}{2r} \cdots\cdots\cdots\cdots\cdots\cdots\cdots (21)$$

Step 3: (Compute the Perturbed Newton Correction)

Solve the reduced correction Eq. (18) for $(\Delta x_k, \Delta y_k)$, then the following equations for $(\Delta l_k, \Delta u_k; \Delta z_k, \Delta w_k)$:

$$\left.\begin{array}{l} \Delta l_k = \nabla g(x)^T \Delta x_k + L_{z0} \\ \Delta u_k = -\nabla g(x)^T \Delta x_k - L_{w0} \\ \Delta z_k = L^{-1}(-Z\Delta l_k - LZe + \mu e) \\ \Delta w_k = U^{-1}(-W\Delta u_k - UWe - \mu e) \end{array}\right\} \cdots\cdots (22)$$

The perturbed Newton correction Δv_k is:

$$\Delta v_k = [\Delta x_k, \Delta l_k, \Delta u_k; \Delta y_k, \Delta z_k, \Delta w_k]^T$$

Step 4: (Determine the Maximum Step Length)

Perform the ratio test to determine the maximum primal and dual step lengths that can be taken in the Newton direction:

$$\left.\begin{array}{l} \theta P_k \\ = \min\left\{\min_m\left(\frac{-l_m}{\Delta l_m} : \Delta l_m < 0; \frac{-u_m}{\Delta u_m} : \Delta u_m < 0\right), 1\right\} \\ \theta D_k \\ = \min\left\{\min_m\left(\frac{-z_m}{\Delta z_m} : \Delta z_m < 0; \frac{-w_m}{\Delta w_m} : \Delta w_m > 0\right), 1\right\} \\ (m = 1, 2, \cdots, r) \end{array}\right\} \cdots\cdots\cdots\cdots (23)$$

Form the step length matrix:

$$\Theta_k = 0.99 diag[\theta P_k, \cdots, \theta P_k; \theta D_k, \cdots, \theta D_k]$$

The scalar 0.99 is a safety factor to ensure that the next point will satisfy the strict non-negativity conditions imposed on the slack variables.

Step 5: (Update Variables)

Update the primal and dual variables by:

$$v_{k+1} = v_k + \Theta_k \Delta v_k \cdots\cdots\cdots\cdots\cdots\cdots (24)$$

then return to Step 1.

End

5.4 Choice of Initial Values In Dynamic TTC solution, it has been observed that the above algorithm is not quite sensitive to the selection of the initial values. By setting the initial values of the control variables as the averages of their two limits and calculating initial rotor angle δ_i^0 and constant voltage E_i' by Eq. (8), the algorithm can converge to the optimal solution satisfactorily. In this study, the initial values are chosen as follows:

(a) Primal Variables $x^{(0)}$:
Voltages: $V_i^{(0)} = 1$, $\theta_i^{(0)} = 0$
Controllable active power outputs:
$P_{gi}^{(0)} = (\underline{P}_{gi} + \bar{P}_{gi})/2$
Controllable reactive power outputs:
$Q_{gi}^{(0)} = (\underline{Q}_{gi} + \bar{Q}_{gi})/2$
Rotor speed: $\omega_i^{(0)} = \omega_0$
Rotor angle: δ_i^0 is determined by Eq. (8)

(b) Slack Variables $l^{(0)}$ *and* $u^{(0)}$:
$l^{(0)} = g(x^{(0)}) - \underline{g}$, $u^{(0)} = \bar{g} - g(x^{(0)})$

(c) Dual Variables $z^{(0)}$, $w^{(0)}$ *and* $y^{(0)}$:
$y^{(0)} = 10^{-8}$; $z^{(0)} = 1$, $w^{(0)} = -1$

6. Test Results and Discussions

In this section, we give some test results to verify the effectiveness of the proposed D-ATC evaluation method. For the convenience of future practical application, our dynamic TTC calculation program is written in FORTRAN. It has been tested on several test systems. In order to help other researchers to crosscheck the results, in this paper we present the results of two public domain systems—IEEJ WEST10 model system and IEEJ WEST30 model system [10]. The standard data of both systems can be obtained from the following IEEJ specified website:

http://www.pwrs.elec.waseda.ac.jp/powsys/

6.1 Test Results of IEEJ WEST10 Model System

(a) System illustration and simulation conditions
IEEJ WEST10 Model System, which has 10 machines and 27 buses, is a simplified modeling of the 60 Hz power system in Japan. One-line diagram of the system is shown in Fig. 3.

As an example, we present an simulation example in which the objective is to determine the maximum real power transfer from areas which have cheaper coal power (G1∼G3) to those areas where high price natural gas are used through the transfer path (L40). We construct two cases:

Case-1: S-ATC without transient stability constraints
Case-2: D-ATC with transient stability constraints

For D-ATC, we assume that the contingency is a three-phase-to-ground fault (3LG-O), which occurs at 0.1 s and is cleared 70 ms later by the opening of one of the double line, at the sending end of line 40 (position D). The transient stability limit is set as the maximum relative rotor angle w.r.t. center of inertial (COI) 100 degree. The integration step-width Δt is fixed to be 0.01 s and the maximum integration period $T_{\max}$ is set to be 2.0 s.

For the calculating accuracy of the solution, in all cases, in order to check whether a step-width as large as 0.01 s is suitable, dynamic responses obtained by our D-ATC are verified by the widely-used CRIEPI's Power System Dynamic Stability Analysis Program, which use the optimal solution given by D-ATC as operating point and set the step-width as 0.001 s. The results are fairly well identical. This not only guarantees that D-ATC solution has high accuracy, also demonstrates that a step-width as large as 0.01 s is suitable.

(b) Effectiveness of the proposed dynamic TTC formulation If we don't include a transient stability constraint, which is in steady-state ATC, the TTC of transmission path L40 is 5604 MW. However, the system is unstable after contingency D. On the other hand, D-ATC ensures transient stability at the expense of decreasing the TTC to 3608 MW. Fig. 4 compares the relative rotor angle behavior of S-ATC and D-ATC. From this result we can clearly see that transient stability is ensured only when the related constraints are incorporated into ATC.

Fig. 5 shows how the TTC changes with the stability limits. As is shown in Fig. 5, a stricter rotor angle limit restricts TTC more heavily. Although this conclusion is straightforward, it is very meaningful. It implies that when transmission companies are willing to take stability risk they can incur greater profit. Furthermore, we think that it is possible to use the limit of rotor angles w.r.t. COI as an index for pricing dynamic security in nowadays deregulated power market. However, this still need further detailed study.

(c) Efficiency of the proposed solution algorithm
Dynamic TTC is a large-scale nonlinear programming

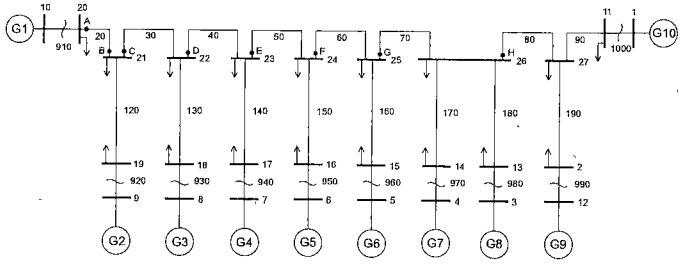

Fig. 3. IEEJ WEST10 model system

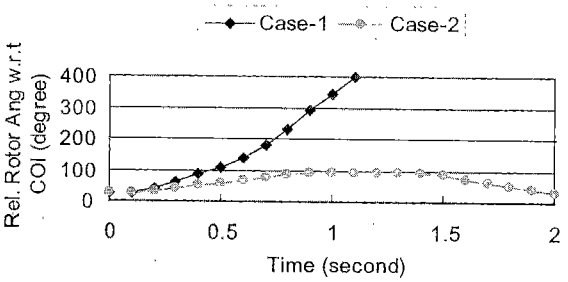

Fig. 4. Relative rotor angle behavior (WEST10)

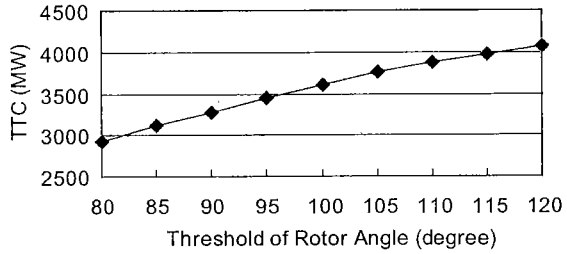

Fig. 5. TTC with limit of rotor angle w.r.t. COI (degree)

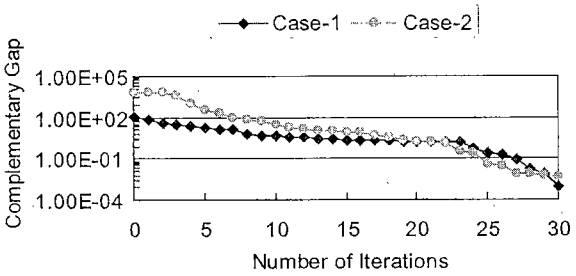

Fig. 6. Complementary gap with iterations (WEST10)

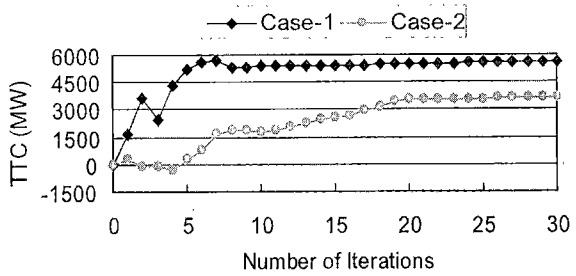

Fig. 7. TTC with iterations (WEST10)

problem. In the above Case-2, it needs to coordinate more than 16,000 primal-dual variables to search for the optimal solution. Even for this extremely large problem, the proposed solution is fast enough to converge to the optimal result in less than 30 seconds by an IBM Pentium III-1 GHz computer.

Moreover, the proposed solution algorithm has excellent convergence characteristic. When using primal-dual Newton IPM to solve dynamic TTC problems, convergence condition is that complementary gap is smaller than a defined tolerance. Thus complementary gap is a very important measure to judge the optimality of solutions and its change reflects the characteristic of the algorithm. Fig. 6 shows how it reduced with iterations for the above two cases. We can see it decreases to zero monotonically and rapidly. Fig. 7 shows how the TTC changes with iterations. In both cases, the convergences to optimal solutions are quite smooth.

6.2 Test Results of IEEJ WEST30 Model System In above subsection 6.1, we have demonstrated the effectiveness of the proposed dynamic TTC formulation as well as its solution algorithm by the simulation results of IEEJ WEST10 model system. In this subsection, simulation results of IEEJ WEST30 model system are presented to illustrate that the proposed method is suitable for large-scale system application.

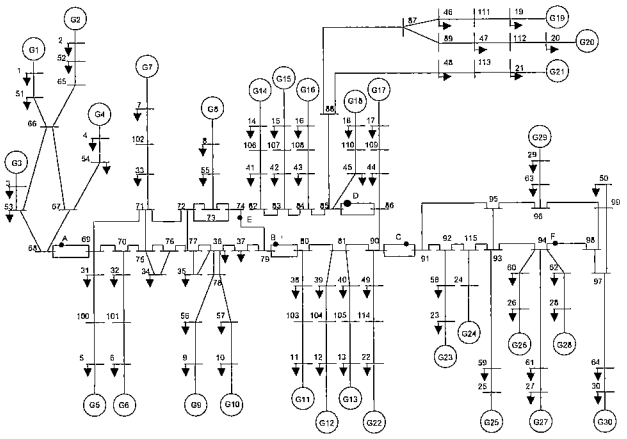

Fig. 8. IEEJ WEST30 model system

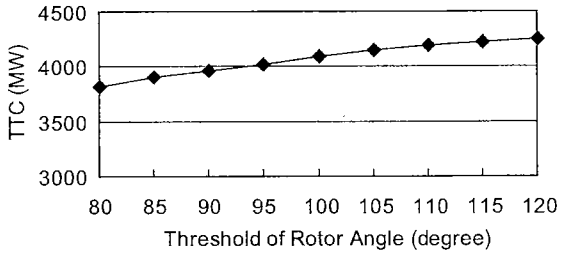

Fig. 9. TTC with limit of rotor angle w.r.t. COI (WEST30).

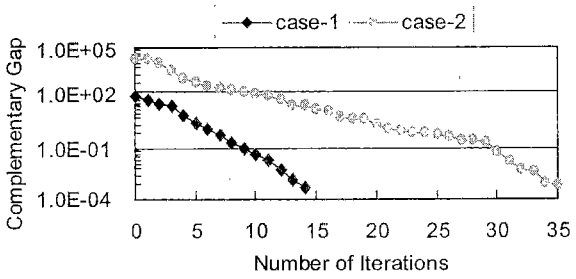

Fig. 10. Complementary gap with iterations (WEST30)

Based on the reduction of the real system, IEEJ WEST30 model system reflects the characteristics of the Japanese 60 Hz power system more closely than IEEJ WEST10 model system. IEEJ WEST30 model system has 30 machines, 115 nodes, 129 branches. Fig. 8 shows the one-line diagram of this system.

Similar to the simulation of IEEJ WEST10 model system, we also construct two cases for IEEJ WEST30 model system: a S-ATC case (Case-1) and a D-ATC case (Case-2). As an example, we assume that western part of the system has low cost power and calculate the TTC from node 79 to node 80. For Case-2, the contingency is a 3LG-O at position B.

In S-ATC, the TTC of transmission corridor 79–80 is up to 5480 MW. While in D-ATC, owing to the limitation of stability constraints, TTC decreases considerably. Fig. 9 shows how the TTC changes with stability limits.

Fig. 10 and Fig. 11 depict the convergence characteristics of Case-1 and Case-2. In Case-2 the stability limit is 105 degree. We can see that the proposed solution

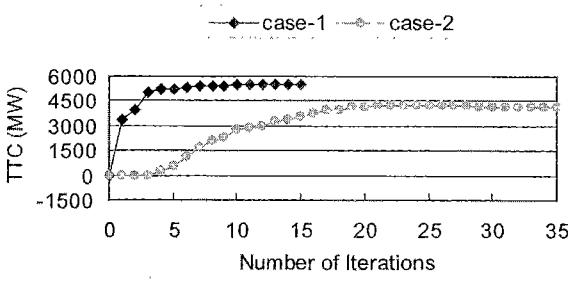

Fig. 11. TTC with iterations (WEST30)

algorithm has perfect convergence even for this large problem, in which more than 48,000 primal-dual variables need to coordinate to search for the optimal solution.

For the convergence of the optimization solution, we find that interior point nonlinear programming algorithm has perfect convergence characteristic. In our studies on transient stability related optimization problems using interior point nonlinear programming, we always obtain excellent solution.

7. Conclusions

Successful implementation of electric power deregulation requires the determination of the ATC of a power system. In this paper, first, a novel method for integrating transient stability constraints into ATC problem was presented. Then, the dynamic ATC problem was successfully formulated as an OPF-based optimization problem. Finally, a solution of dynamic TTC by the primal-dual Newton IPM for NLP problems was proposed.

The effectiveness of the dynamic TTC formulation and the solution algorithm was demonstrated on the IEEJ WEST10 and IEEJ WEST30 model systems.

It is important to consider multi-contingencies in D-ATC calculation. In fact, our present D-ATC program has been designed to include multi-contingencies. However, the problem is how to pick out "binding contingencies". This is a future work of D-ATC method.

(Manuscript received June 5, 2002,
revised June 17, 2003)

References

(1) Power Systems Engineering Research Center: Electric Power Transfer Capability: Concepts, Applications, Sensitivity and Uncertainty, No.01-34, PSERC Publication (2001-11)

(2) S. Repo: "Real-time Transmission Capacity Calculation in Voltage Stability Limited Power System", Proc. of Bulk Power System Dynamics and Control IV—Restructuring, pp.599–605, Santorini, Greece (1998-8)

(3) I.A. Hiskens, M.A. Pai, and P.W. Sauer: "Dynamic ATC", Proc. of the 2000 IEEE Power Engineering Society Winter Meeting, Singapore (2000-1)

(4) Transmission Transfer Capability Task Force: "Available Transmission Capability Definitions and Determination", North American Electric Reliability Council (NERC), Princeton, New Jersey (1996-6)

(5) M.A. Pai: Power System Stability, North-Holland Publishing Company (1981)

(6) B. Stott: "Power System Dynamic Response Calculations", *Proc. IEEE*, Vol.67, No.2, pp.219–241 (1979)

(7) T. Athay, R. Podmore, and S. Virmani: "Practical Method for the Direct Analysis of Transient Stability", *IEEE Trans. PAS*, Vol.98, No.2, pp.573–584 (1979)

(8) Y. Yamada, M. Nagata, and K. Tanaka: "Contingency Screening Method for ATC Assessment with Transient Stability Constraints", 2002 National Convention Record IEE Japan, 6-001 Tokyo (2002-3)

(9) A.S. El-Bakry, R.A. Tapia, T. Tsuchiya, and Y. Zhang: "On the Formulation and Theory of the Newton Interior-Point Method for Nonlinear Programming", *J. Opt. Theory & Applications*, Vol.89, No.3, pp.507–541 (1996)

(10) IEEJ Technical Committee: "Standard Models of Power Systems", Technical Report, IEE Japan, No.754 (1999-11)

(11) D. Gan, R.J. Thomas, and R.D. Zimmerman: "A Transient Stability Constrained Optimal Power Flow", Bulk Power System Dynamics and Control IV—Restructuring, Santorini, Greece (1998)

(12) L. Chin, A. Ono, Y. Toda, H. Okamoto, and R. Tanabe: "Optimal Operation of Power System Constrained by Transient Stability", *T. IEE Japan*, Vol.120-B, No.12, (2000-12)

(13) S. Fujiwara and A. Yokoyama: "Available Transmission Capacity Index Considering Various Kinds of Stability", The Papers of Technical Meeting on Power Engineering and Power System Engineering, IEE Japan, PE-98-101 (1998)

(14) M. Nagata, M. Takemura, T. Okada, and K. Tanaka: "Development of ATC Assessment System", Proc. of 2002 Annual Conference of Power & Energy Society, IEE Japan, pp.501–502 (2002)

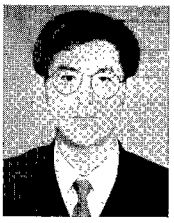

Yue Yuan (Member) was born in Xi'an, China, on March 29, 1966. He received the B.S. and M.S. degrees in electrical engineering from Xi'an Jiaotong University, China, in 1987 and 1990, respectively. He received the Ph.D. degree from Hiroshima University, Japan in 2002. He joined the faculty of Xi'an Jiaotong University, China, in 1990. He was in Hiroshima University from 1998 to 2002. Currently, he is a Professor of Hohai University, China. His research interests include power system operations and optimization. Dr. Yuan is a member of the IEEJ.

Junji Kubokawa (Member) was born in Hiroshima, Japan, on January 11, 1965. He received the B.S. degree from Hiroshima Institute of Technology, Japan, in 1987, the M.S. and Ph.D. degrees from Hiroshima University, Japan, in 1989 and 1999 respectively. He was an Academic visitor of Imperial Collage Science, Technology and Medicine from 1993 to 1995. He had been Lecturer of Hiroshima University, Japan, from 1989 to 2001. Now, he is an Associate Professor of Hiroshima Institute of Technology, Japan. His research interest is in power system operation and planning, particularly in the application of optimization methods to power systems. Dr. Kubokawa is a member of the IEE of Japan.

Hiroshi Sasaki (Member) was born in Hiroshima, Japan, on March 10, 1941. He received the B.S., M.S., and Ph.D. degrees in electrical engineering from Waseda University, Tokyo, Japan, in 1963, 1965, and 1979, respectively. He is a Professor in the Department of Electrical Engineering, Hiroshima University, Japan. He was given visiting Lectureship from the University of Salford, Salford, England, from 1971 to 1972. He was a visiting Professor at the University of Texas, Arlington, from 1984 to 1985. He has been studying various problems in power engineering field especially expert systems and artificial neural network application to power systems, etc. Dr. Sasaki is a member of CIGRE, the IEE of Japan, and the Atomic Energy Society of Japan.